Available online at www.sciencedirect.com
SCIENCE DIRECT
Chemical Physics 324 (2006) 489–496
Chemical Physics
www.elsevier.com/locate/chemphys

Spectral and structural study of two acceptor-substituted pyridinium-betaines of squaric acid: Promising chromophores for nonlinear optical applications

Tsonko Kolev *, Bistra Stamboliyska, Denitsa Yancheva

Institute of Organic Chemistry, Bulgarian Academy of Sciences, 1113 Sofia, Bulgaria

Received 15 July 2005; accepted 17 November 2005
Available online 20 December 2005

Abstract

Two acceptor-substituted chromophores (3- and 4-benzoylpyridinium-betaines of squaric acid) were characterized by means of thermogravimetric analysis and UV–vis and IR spectra. The experiment is supported by theoretical predictions undertaken at different levels of approximation (MP2 and DFT/B3LYP). The results of the optimized molecular structure are presented and compared with the X-ray diffraction data for both chromophores studied. Generalized atomic polar tensor (GAPT) model was chosen for calculation of atomic charges of studied species. The charge distribution over fragments indicates that strongly polarized systems are present. Harmonic vibrational frequencies of the molecules were evaluated theoretically using B3LYP/6-311G** level. The nonlinear optical efficiency of both chromophores was estimated by molecular parameters such as absorption maxima in various solvents of different polarity, ground state dipole and difference between ground and excited state dipole moments. A static hyperpolarizability for 4-benzoyl chromophore was provided from EOAM experiment for a dioxane solution. Combined with the noncentrosymmertic crystal structure of the same isomer and the exceptional thermal stability of both species, these studies gave evidences for their reliability as nonlinear optical materials.

Keywords: Organic materials for nonlinear optics; UV–vis; IR; Molecular design; MP2; DFT

1. Introduction

The rapidly growing interest to the organic nonlinear optical (NLO) materials inspired investigation of various chemical species mainly long chain push–pull polyenes, merocyanines, ionic and compounds with internal charge separation [1,2].

It has been long recognized that the electronic structure and the strength of donor and acceptor groups are responsible for achieving large molecular hyperpolarizabilities (β). Optimization of β on molecular level is directed towards synthesis of chromophores exhibiting intense low-lying absorption maxima with high dipoles of the charge transfer transition (μ_{ag}) and large difference between ground and excited state dipole moments ($\Delta\mu$). These molecular parameters could be used as characteristics for their NLO potential [1,2].

UV–vis electronic absorption and vibrational spectroscopical measurements are widely employed as complementary experimental techniques to provide important information on the molecular hyperpolarizabilities [3–5]. Additionally, using quantum chemical calculations is a field of intense research because of its relevance to the full understanding of the relationship between structure and NLO efficiency [3,6–8].

However, the role of the crystal structure is crucial in the building-up of the bulk nonlinearity of the materials as it was demonstrated by numerous crystallographic studies [9–14]. Only noncentrosymmetric alignment of the chromophores in the crystal lattice leads to an observable bulk second-order NLO response.

* Corresponding author. Tel.: +359 2 9606106; fax: +359 2 8700225.
E-mail address: kolev@orgchm.bas.bg (T. Kolev).

0301-0104/$ - see front matter © 2005 Elsevier B.V. All rights reserved.
doi:10.1016/j.chemphys.2005.11.014

The pyridinium-betaines of squaric acid (PB) represent a novel class of internally charged systems whose promising properties for potential NLO application were first reported in 2001 [15].

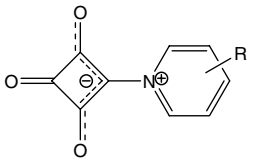

R = 3-COC_6H_5 (3BzPB)

R = 4-COC_6H_5 (4BzPB)

R = 4-$N(CH_3)_2$ (DAPB)

(PB)

These zwitterionic chromophores combine large molecular ground state dipole moments for relatively small molecules, low-lying highly intense absorption maxima in the visible region, and easy way of varying the donor–acceptor strength of the conjugated system.

Recently many spectral and theoretical [16–18] as well as structural [19–22] studies were devoted to characterizing their properties. The molecular hyperpolarizabilities of six main representatives of the series were determined by electro-optical absorption measurements (EOAM) [23].

In this paper we focus on the electronic and vibrational spectra, both in solid state and in a variety of solvents, of two acceptor substituted PB: 3-benzoylpyridinium-betaine of squaric acid (3BzPB) and 4-benzoylpyridinium-betaines of squaric acid (4BzPB). Since the characterization of the molecular conformation and the charge distribution of the chromophores studied are essential to complete understanding its NLO properties, we used DFT and MP2 in order to perform structural analysis and to predict IR spectra. These results were then used to interpret the observed vibrational spectra of the studied molecules.

2. Experimental and computations methods

The FTIR spectra were measured in solid state as KBr, CsI and polyethylene pellets on a Bruker IFS-113v FTIR spectrometer equipped with a high intensity Globar source, Ge/KBr beam splitter and DTGS detector in the middle infrared region. The FIR spectra were recorded with the same spectrometer using a high pressure Hg arc lamp and a 6-μm Mylar beam splitter and DTGS detector. In all cases the spectra were recorded at a resolution of 1 cm^{-1} (200 scans).

The TG-DTG (thermogravimetric analysis) investigations were performed in a Setaram TG92 instrument. One hundred milligrams of the sample was placed in a microbalance crucible and heated in a flow of Ar (70 cm^3/min) up to 623 K at 8 K/min.

The quantum chemical calculations were performed with GAUSSIAN-98 program package [24]. The geometries of both chromophores were optimized at two level of theory: second-order Møller–Pleset perturbation theory (MP2) and density functional theory, using the 6-311G** basis set. The DFT method employed in this work is B3LYP, which combines Becke's three – parameter nonlocal exchange with the correlation functional of Lee, Yang and Parr [25,26]. Molecular geometries of studied species were fully optimized by the force gradient method using Bernys' algorithm [27]. For every structure, the stationary points found on the molecular potential energy hypersurfaces were characterized using standard analytical harmonic vibrational analysis. The absence of imaginary frequencies, as well as of negative eigenvalues of the second-derivative matrix, confirmed that the stationary points correspond to minima on the potential energy hypersurfaces. The geometries of the NLO-phores in the lowest singlet excited state were optimized using the configuration interaction singles (CIS) procedure. To estimate the difference between the dipole moments in ground and excited state of the studied molecules, we have performed the population analysis using the CI (CI-singles) density and the SCF (ground state) density by including the key word density = CI.

The calculated vibrational frequencies and infrared intensities were used to assist the analysis of the experimental spectra. In order to check statistically which kind of calculation performed agrees best with the experimental vibrational data for the species studied, we have treated the correlation between their theoretical and experimental IR frequencies. In this case DFT method provided more accurate vibrational data. The calculated standard deviations are 11 cm^{-1} (B3LYP) and 21 cm^{-1} (MP2) for 4BzPB and 12 cm^{-1} (B3LYP) and 26 cm^{-1} (MP2) for 3BzPB, respectively. So, we will use just B3LYP/6-311G** data in the analysis of the IR data. For a better correspondence between experimental and calculated values, we modified the results using the empirical scaling factors (0.9614), reported by Scott and Radom [28].

3. Results and discussion

3.1. Synthesis and UV–vis spectra

The condensation of squaric acid with equimolar amounts of substituted pyridines gives the corresponding pyridinium-betaines of squaric acid as described by the general procedure of Schimdt et al. [29]. Boiling the reagents in acetic anhydride affords the monocondensation products in good yields as crystalline compounds. The synthesis of 4BzPB and 3BzPB is given in detail in our previous paper [18].

The electronic-structure characterization of compounds with internal charge separation is impossible without knowing their UV–vis absorption behaviour. Moreover, important information on the intensity and the energy of their CT transition could be derived by UV–vis analysis.

The absorption maxima of compounds studied in 1,4-dioxane, 1,2-dichloroethane, 1-methylpyrrolidin-2-one, acetonitrile, ethanol and water as well as the normalized

Reichardt's parameters [30] for the polarity of the solvents employed are listed in Table 1. For the purpose of comparing the solvatochromic behaviour and the substituent effects the absorption maxima of the donor substituted DAPB are also given in the table.

All the three compounds exhibit negative solvatochromism typical for molecules with dipolar ground state structure. Concerning the influence of donor and acceptor groups, a bathochromic shift of the absorption of 4BzPB and 3BzPB in comparison to DAPB is observed in all the solvents employed. Obviously, the dipolar ground state structure of the two isomers is stabilized by the presence of acceptor benzoyl group, but the stabilizing effect is weaker for the group being in 3-position, which is in accordance with the general views about the substituent effects. Increasing the positive charge on the N-atom the acceptor group favours the CT and thus the negative solvatochromism is more strongly expressed (Table 1).

3.2. Molecular structure

The optimized structures of 4BzPB and 3BzPB are depicted in Schemes 1 and 2, respectively.

According to the quantum chemical calculations two distinct stable conformations for 3BzPB exist differing by internal rotation around the bond C^9–C^{11} (see Scheme 2): I (*syn*, C^{10}–C^9–C^{11}=O, 149°) and II (*anti*, C^{10}–C^9–C^{11}=O, 32°). When energies are corrected by zero point vibrational energy contribution, both B3LYP and MP2 calculation predict form I as being more stable with 6 kJ mol^{-1}. This is indeed the conformation adopted by the molecule of 3BzPB in solid state as determined by single crystal X-ray diffraction [21].

In both isomers the squarate and pyridinium rings are coplanar and twisted not only relative to the carbonyl group but also to the phenyl ring. Further comparison of the geometry of 4BzPB and 3BzPB reveals significant difference within the dihedral angle between the least-squares planes through the six-membered rings, since the mentioned angle in 4BzPB is 77°, whereas the corresponding one in 3BzPB is 50°. These theoretical results are in perfect agreement with the crystallographic data [15,21]. Dihedral angle comparable to this in 3BzPb was previously reported for 4-dimethylamino-4′-nitrobenzophenone [31].

Optimized geometry parameters, i.e., bond lengths and bond angles, computed at the B3LYP and MP2 level are collected together with those found by single crystal X-ray diffraction in Tables 2 and 3, respectively. One can see that the methods used give good descriptions of the geometry of the studied molecules.

Both computation methods predict C^1–O^{14} to be nearly double bond in character, which is in accordance to the single crystal data. The almost identical lengths of the remaining two carbonyl groups in the squaric fragment, namely C^2–O^{13} and C^4–O^{12} indicate that a mesomeric equalization of the bonds takes place. It is interesting to note that MP2 method underestimated the C=O and C–O bond lengths, while B3LYP method gives quite accurate values.

According to earlier studies exploiting some strategies for design of second-order NLO crystals without using chirality [2,32,33] 4BzPB and 3BzPB are supposed to crystallize preferably in noncentrosymmetric space groups due to their structural analogy to substituted benzophenones.

The crystallographic study of 4BzPB [15] and 3BzPB [21] revealed the occurrence of large network of intermolecular interactions stabilizing the three-dimensional packing of the molecules. Some of them involving the pyridinium H-atoms and the negatively charged O-atoms should be considered as nonclassical hydrogen bonds and in the case of 4BzPB link the molecules to form ribbons. In contrast, in the crystal of 3BzPB the molecules are two-dimensionally connected.

Although similar in conformation the two isomers crystallize in different manner – the crystal of 3BzPB is monoclinic and centrosymmetric ($P2_1/n$), whereas 4BzPB crystallizes noncentrosymmetrically in orthorhombic space group $Pna2_1$. To clarify the influence of the highly polar structure of PB on the noncentrosymmertic alignment in the crystal the molecular conformations of the compounds studied should be considered.

The generalized atomic polar tensor (GAPT) model [34] was chosen for calculation of atomic charges of studied species. GAPT charges over fragments for 4BzPB and 3BzPB are shown in Schemes 1 and 2, respectively.

The charge distribution over fragments indicates that a strongly polarized system is present with squaric fragment bearing nearly 80% of the net negative charge of the molecule. The positive charge is equally distributed over the pyridinium ring and the benzoyl C=O group likely due to the effective conjugation between them. In that way the negative and the positive moiety of the molecule prove to be in immediate vicinity without any linking chain

Table 1
UV–vis absorption maxima (λ in nm) of NLO-phores 4BzPB, 3BzPB and DABP in various solvents of different polarity (denoted by the normalized Reichardt's parameter E_T^N in brackets)

Compound	1,4-DX[a] (0.164)	1,2-DCE[b] (0.327)	NMP[c] (0.355)	CH_3CN(0.460)	C_2H_5OH(0.654)	H_2O(1.00)
4BzPB	419	417	400	400	381	–
3BzPB	–	403	391	376	370	352
DAPB	372	369	370	364	357	352

[a] 1,4-DX = 1,4-dioxane.
[b] 1,2-DCE = 1,2-dichloroethane.
[c] NMP = 1-methylpyrrolidin-2-one.

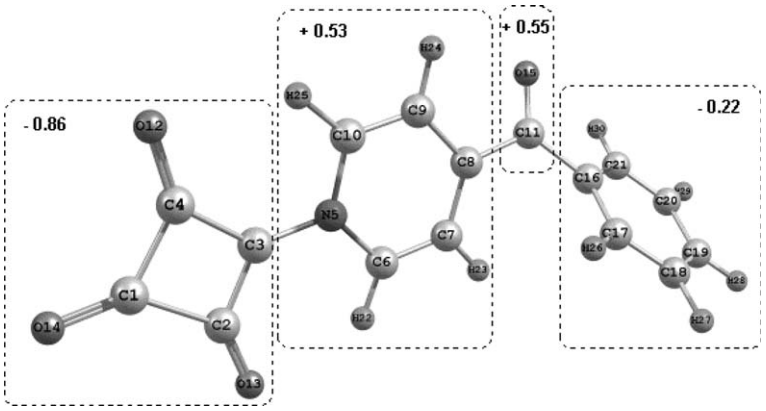

Scheme 1. B3LYP/6-311G** molecular geometry and GAPT charges over the fragments of 4BzPB.

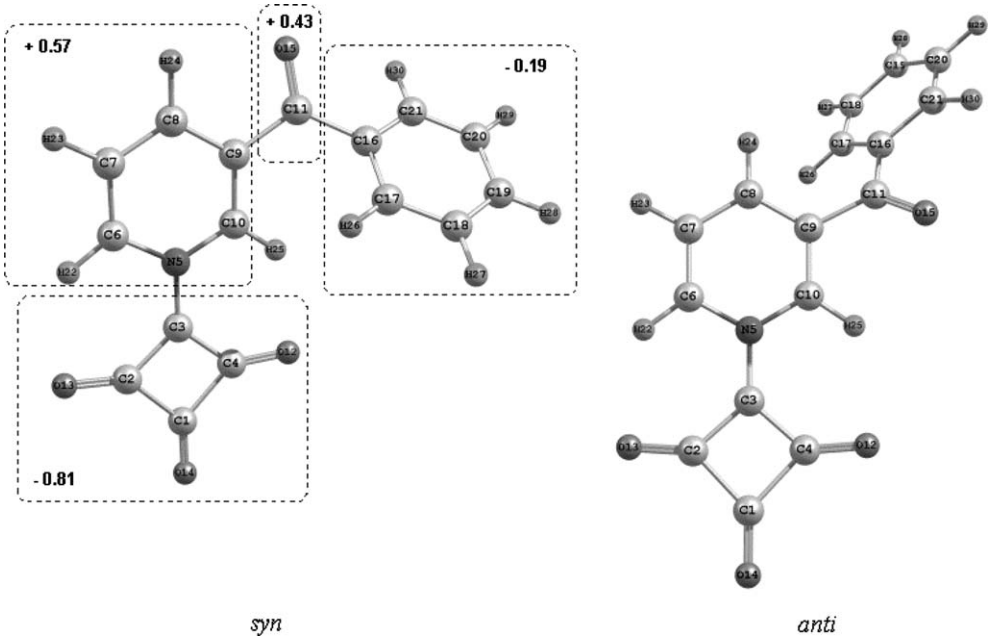

Scheme 2. Relevant conformations of 3BzPB and GAPT charges for more stable *syn* conformer as deduced from B3LYP/6-311G** calculations.

between them which renders impossible determination of bond length alternation (BLA) or characterizing the system by c^2 parameter. This charge distribution results in comparatively high ground state dipole moment (μ_g). μ_g(4BzPB), calculated by means of MP2 and DFT is 10.48 and 10.91 D, respectively. The corresponding values for μ_g(3BzPB) are as follow 9.33 and 9.82 D. The theoretical methods reproduce very well the experimental data for 4BzPB found by EOAM [23] (9.35 D) and based on this good coincidence it could be expected that the dipole moment of 3BzPB is also reliable. It is well known that large difference between the dipoles in ground and excited state of the molecule is a sign of large β [1,2]. We found that excitation causes a decrease of 4.84 and 3.89 D, respectively, in the dipole moments of 4BzPB and 3BzPB. These theoretical assumptions are sustained by the solvatochromic behaviour (reverse charge transfer upon excitation, i.e., from the acceptor to the donor group) of all PB studied by us so far [18]. The static hyperpolarizability (β_0) of 4BzPB estimated in the two-level model [1,2] on the basis of the quantities μ_g, μ_{ag}, and $\Delta\mu$ derived from EOAM for a dioxane solution is -26×10^{-50} CV^{-2} m^3 [23]. This value is higher than β_0 of the classical push–pull molecule *p*-nitroaniline (6×10^{-50} CV^{-2} m^3 [35]) and comparable to β_0 of a number of well-known and efficient NLO-phores for electro-optical and photorefractive applications [36,37]. The large hyperpolarizability combined with the low relative molecular weight of both chromophores and their good transparency properties enable elaboration of crystalline materials and ''organic glasses'' with higher chromophores density.

The zwitterionic nature of these compounds leads to strong interactions in the crystalline state and high melting points. The TG-DTG analysis was carried out for a not

Table 2
Theoretical (B3LYP/6-311G** and MP2/6-31G**) bond lengths (Å) and bond angles (degrees) compared with X-ray data of 4BzPB[a]

	Exp.	B3LYP	MP2		Exp.	B3LYP	MP2
Bond lengths				*Bond angles*			
C^1–C^2	1.532(4)	1.572	1.564	$\angle(C^2C^1C^4)$	88.0(17)	87.3	87.9
C^1–C^4	1.539(4)	1.573	1.564	$\angle(C^2C^1O^{14})$	136.2(3)	136.4	136.1
C^1–O^{14}	1.203(3)	1.200	1.213	$\angle(C^1C^2C^3)$	87.7(2)	87.7	87.5
C^2–C^3	1.421(3)	1.444	1.446	$\angle(C^1C^2O^{13})$	135.1(2)	137.3	137.3
C^2–O^{13}	1.217(4)	1.223	1.231	$\angle(C^2C^3C^4)$	97.0(18)	97.4	97.3
C^3– C^4	1.427(4)	1.445	1.446	$\angle(C^2C^3N^5)$	131.3(3)	131.1	131.2
C^3–N^5	1.404(3)	1.382	1.378	$\angle(C^1C^4C^3)$	87.2(2)	87.6	87.4
C^4–O^{12}	1.223(4)	1.222	1.231	$\angle(C^1C^4O^{12})$	135.2(2)	137.2	135.4
N^5–C^6	1.355(4)	1.370	1.372	$\angle(C^3N^5C^6)$	119.3(2)	119.6	119.3
N^5–C^{10}	1.365(3)	1.374	1.374	$\angle(C^6N^5C^{10})$	121.2(7)	120.6	121.4
C^6–C^7	1.364(4)	1.380	1.381	$\angle(N^5C^6C^7)$	120.3(3)	120.2	119.7
C^7–C^8	1.396(4)	1.404	1.403	$\angle(C^6C^7C^8)$	119.4(3)	120.6	120.5
C^8–C^9	1.382(4)	1.405	1.403	$\angle(C^7C^8C^9)$	119.8(8)	117.8	118.1
C^8–C^{11}	1.512(3)	1.507	1.497	$\angle(C^7C^8C^{11})$	120.3(3)	124.1	123.4
C^9–C^{10}	1.373(4)	1.376	1.379	$\angle(C^8C^9C^{10})$	119.3(2)	120.8	120.7
C^{11}–O^{15}	1.215(4)	1.225	1.236	$\angle(N^5C^{10}C^9)$	120.0(3)	120.0	119.4
C^{11}–C^{16}	1.467(4)	1.492	1.485	$\angle(C^8C^{11}O^{15})$	116.4(3)	118.0	118.9
C^{16}–C^{17}	1.386(4)	1.405	1.404	$\angle(C^8C^{11}O^{16})$	119.7(3)	120.7	119.5
C^{16}–C^{21}	1.399(3)	1.405	1.402	$\angle(C^{15}C^{11}O^{16})$	123.9(2)	121.3	122.0
C^{17}–C^{18}	1.388(4)	1.394	1.395	$\angle(C^{11}C^{16}C^{17})$	121.1(2)	123.0	122.0
C^{18}–C^{19}	1.376(4)	1.396	1.396	$\angle(C^{16}C^{17}C^{18})$	119.8(3)	120.2	119.7
C^{19}–C^{20}	1.372(5)	1.398	1.398	$\angle(C^{17}C^{18}C^{19})$	119.9(3)	120.0	120.2
C^{20}–C^{21}	1.374(5)	1.391	1.392	$\angle(C^{18}C^{19}C^{20})$	120.7(3)	120.1	120.1

[a] For atom numbering see Scheme 1.

Table 3
Theoretical (B3LYP/6-311G** and MP2/6-31G**) bond lengths (Å) and bond angles (degrees) compared with X-ray data of 3BzPB[a]

	Exp.	B3LYP	MP2		Exp.	B3LYP	MP2
Bond lengths				*Bond angles*			
C^1–C^2	1.533(4)	1.571	1.563	$\angle(C^2C^1C^4)$	88.2(2)	87.2	87.8
C^1–C^4	1.527(5)	1.574	1.564	$\angle(C^2C^1O^{14})$	136.2(2)	136.4	136.1
C^1–O^{14}	1.204(4)	1.194	1.213	$\angle(C^1C^2C^3)$	87.8(2)	87.7	87.3
C^2–C^3	1.430(4)	1.441	1.445	$\angle(C^1C^2O^{13})$	135.4(2)	137.1	137.3
C^2–O^{13}	1.219(3)	1.217	1.231	$\angle(C^2C^3C^4)$	96.5(3)	97.6	97.6
C^3–C^4	1.426(4)	1.443	1.446	$\angle(C^2C^3N^5)$	131.5(3)	130.8	131.4
C^3–N^5	1.404(4)	1.386	1.379	$\angle(C^1C^4C^3)$	87.4(2)	87.5	87.3
C^4–O^{12}	1.220(4)	1.214	1.231	$\angle(C^1C^4O^{12})$	135.4(3)	137.0	137.4
N^5–C^6	1.357(4)	1.372	1.368	$\angle(C^3N^5C^6)$	119.8(3)	119.2	119.4
N^5–C^{10}	1.355(4)	1.365	1.368	$\angle(C^6N^5C^{10})$	121.7(3)	120.1	120.8
C^6–C^7	1.378(5)	1.382	1.385	$\angle(N^5C^6C^7)$	120.4(3)	120.0	119.3
C^7–C^8	1.356(5)	1.395	1.399	$\angle(C^6C^7C^8)$	119.8(3)	120.3	120.5
C^8–C^9	1.398(4)	1.399	1.399	$\angle(C^7C^8C^9)$	121.1(3)	119.2	118.9
C^9–C^{11}	1.498(4)	1.514	1.509	$\angle(C^8C^9C^{11})$	120.1(3)	123.5	118.6
C^9–C^{10}	1.374(4)	1.385	1.388	$\angle(C^8C^9C^{10})$	117.9(3)	119.3	119.9
C^{11}–O^{15}	1.216(4)	1.214	1.233	$\angle(N^5C^{10}C^9)$	120.4(3)	120.6	119.5
C^{11}–C^{16}	1.478(4)	1.491	1.482	$\angle(C^9C^{11}O^{15})$	118.9(3)	118.3	117.9
C^{16}–C^{17}	1.389(4)	1.402	1.403	$\angle(C^9C^{11}C^{15})$	120.4(3)	119.9	119.6
C^{16}–C^{21}	1.394(4)	1.405	1.391	$\angle(C^{11}C^{16}C^{17})$	120.0(3)	117.7	122.3
C^{17}–C^{18}	1.377(4)	1.394	1.403	$\angle(C^{16}C^{17}C^{18})$	120.3(3)	120.3	119.7
C^{18}–C^{19}	1.385(5)	1.396	1.394	$\angle(C^{17}C^{18}C^{19})$	120.0(3)	120.0	120.1
C^{19}–C^{20}	1.374(5)	1.396	1.396	$\angle(C^{18}C^{19}C^{20})$	120.0(3)	120.1	120.1
C^{20}–C^{21}	1.379(5)	1.405	1.398	$\angle(C^{19}C^{20}C^{21})$	120.0(3)	120.1	120.2

[a] For atom numbering see Scheme 1.

recrystallized sample of 4BzPB and a recrystallized from DMSO sample of 3BzPB – the corresponding DTG curves are illustrated in Fig. 1. Both samples showed no weight loss as high as 280 °C for 4BzPB and 253 °C for 3BzPB, respectively. After these points a sharp step (loss of more than 65% of weight for both samples) was detected in the TG profiles (not shown) indicating that decomposition process occurred. The corresponding DTG curves are char-

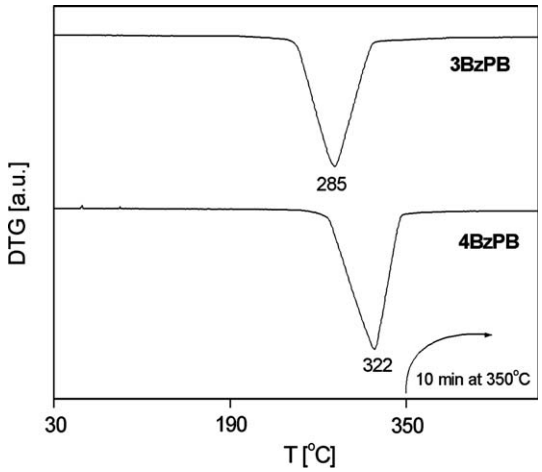

Fig. 1. DTG curves of 3BzPB and 4BzPB.

acterized with maxima at 322 °C for 4BzPB and 285 °C for 3BzPB (Fig. 1). These thermogravimetric data demonstrated good thermal stability for both compounds studied, exceeding by far the typical melting point range of the most well-known NLO molecular crystals (below 150 °C). The higher decomposition point of 4BzPB is most probably due to the above discussed occurrence of extremely large number of short contacts in the crystal.

3.3. Experimental and theoretical IR spectra

The comparison between the experimental spectra of 4BzPB and 3BzPB and the corresponding calculated spectra for the middle IR region is shown in Figs. 2 and 3, respectively. Examination of Figs. 2 and 3 reveals that the experimental IR spectra (KBr pellets) of studied compounds are in general similar to these based on quantum chemical calculations for isolated molecule as well as to each other. The computed vibrational data were used to

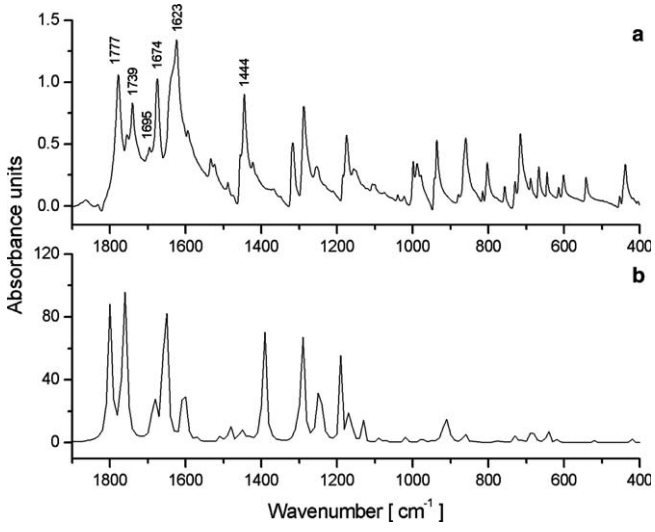

Fig. 2. (a) Experimental (KBr) and (b) calculated (B3LYP/6-311G**) IR spectra of 4BzPB molecule.

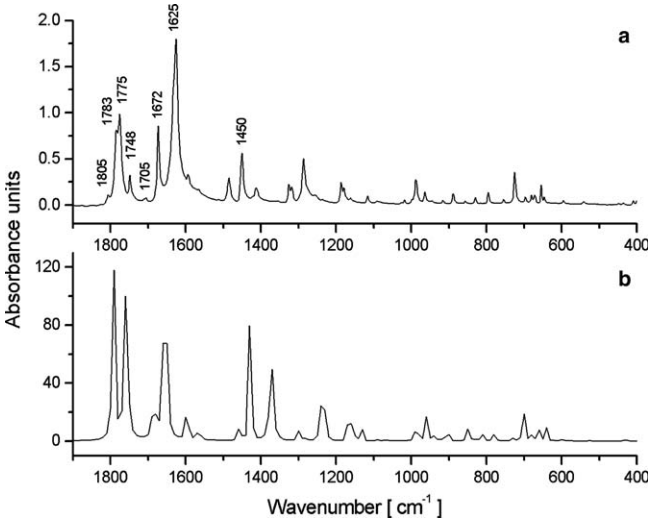

Fig. 3. (a) Experimental (KBr) and (b) calculated (B3LYP/6-311G**) IR spectra of 3BzPB molecule (conformation: I, *syn*).

determine the types of molecular motions associate with each of the observed experimental bands. Tables S1 and S2 (in Supporting Information) present the numeric values of measured frequencies together with calculated B3LYP/6-311G** frequencies and intensities of 4BzPB and 3BzPB, respectively. These tables also list the proposed assignments in detail. For simplicity and taking into consideration the similarity of 4BzPB and 3BzPB in spectra and assignments, the discussion below will be held envizaging both of them.

The frequency region of 1800–1700 cm^{-1} contains in general four intensive carbonyl modes highly characteristic for the substituted PB. Their assignment is less straightforward because more bands appear in the experimental spectrum than expected from the normal modes predicted by the calculations. The stretching vibration of the "pure" carbonyl group – ν_{Sq}(C═O) appears as strong band at the highest frequency in this region. Two bands are present for the mutually connected oscillators C_2O_{13} and C_4O_{12} corresponding to their symmetric ν^{s}(CO) (at around 1740 cm^{-1}) and antisymmetric ν^{as}(CO) (at around 1670 cm^{-1}) stretching vibrations. In Figs. 2 and 3 one can see the observed splitting of ν_{Sq}(C═O) and ν^{s}(CO). All the three carbonyl frequencies of the squaric fragment are lowered compared to the unsubstituted PB [16]. The band of benzoyl C═O stretching appears between ν^{s}(CO) and ν^{as}(CO) (at around 1700 cm^{-1}) and it is shifted by 20 cm^{-1} to the higher frequencies in comparison with 4-benzoylpyridine [38]. Such a shift is reasonably expected as a result of the quaternization of the N-atom and the subsequent positive charging of the benzoyl C-atom.

The normal modes of predominantly ring C–C stretching character (1630–1440 cm^{-1}) are clearly divided into phenyl and pyridinium vibrations (see Table S1 and S2 in Supporting Information). The strongest band in the experimental IR spectrum was assigned to vibration 8a (Wilson' notation). The unusual high intensity of this band in the IR

spectra of PB has already been discussed previously [16,17] in relation to the spectral appearance of some vibrations having form of aromatic-quinone structure transition [39,40].

The intensive band at around 1400 cm^{-1} was assigned as $N–C_{Sq}$ stretching. Its essentially higher frequency than the observed value for other similar pyridinium-betaines [41] is due to the partially quinoide character of this bond.

4. Conclusions

We have investigated two acceptor-substituted pyridinium betaines of squaric acid which are promising candidates for nonlinear optical and electro-optical applications. Their exceptional thermal stability, much higher than the expected for organic molecular crystals, was determined by TG-DTG investigations.

The compounds were analyzed by means of UV–vis and IR spectroscopy. In addition, the structure and harmonic vibrational frequencies of these molecules were theoretically evaluated using MP2 and B3LYP density functional methods. The electronic structure characterization of the compounds studied showed that the presence of acceptor substituent favours the charge transfer and red shifts the absorption maxima. On the basis of the established electronic structure, the large difference between the dipole moments in a ground and an excited state for both chromophores and their intense low-lying absorption maxima in the visible UV region, large molecular hyperpolarizabilities could be expected as proved by the provided experimental value.

All experimental and theoretical data demonstrated the NLO potential of both chromophores studied and the advantage of 4BzPB in terms of its noncentrosymmertic crystal which is prerequisite for the observation of bulk second-order hyperpolarizabilities and makes it suitable for applications based on second- and higher order nonlinear optical processes.

Acknowledgements

T.K. and D.Y. thank to the DAAD and the Alexander von Humboldt Foundation for a grant within the priority program ‘‘Stability Pact for South-Eastern Europe’’. This work has been supported by Bulgarian National Fund of Scientific Research Contracts X-1510. The authors thank to Dr. M. Dimitrov (laboratory ‘‘Organic Reactions on Microporous Materials’’ at the Institute of Organic Chemistry, BAS) for the TG-DTG analysis and helpful discussion.

Appendix A. Supplementary data

Supplementary data associated with this article can be found, in the online version, at doi:10.1016/j.chemphys.2005.11.014.

References

[1] J. Wolff, R. Wortmann, Adv. Phys. Org. Chem. 32 (1999) 121.
[2] H. Nalwa, S. Miyata, in: H. Nalwa, S. Miyata (Eds.), Nonlinear Optics of Organic Molecules and Polymers, CRC Press. Inc., Boca Ratton, 1997 (Chapter 4).
[3] D.M. Bishop, Adv. Chem. Phys. 104 (1998) 1.
[4] M. Lanata, C. Bertarelli, M.C. Gallazzi, A. Bianco, M. Del Zoppo, G. Zerbi, Synth. Met. 138 (2003) 357.
[5] M. Delgado, V. Hernandez, J. Casado, J. Navarrete, J.-M. Raimundo, P. Blanchard, J. Roncali, Chem. Eur. J. 9 (2003) 3670.
[6] H.S. Nalwa, T. Watanabe, S. Miyata, Opt. Mater. 2 (1993) 73.
[7] B. Champagne, D. Bishop, Adv. Chem. Phys. 126 (2003) 41.
[8] R.M. Martin, G. Ortis, Phys. Rev. B 56 (1997) 1124.
[9] P.G. Lacroix, J.C. Daran, K. Nakatani, Chem. Mater. 10 (1998) 1109.
[10] M. Ravi, P. Gangopadhyay, D.N. Rao, S. Cohen, I. Agranat, T.P. Radhakrishnan, Chem. Mater. 10 (1998) 2371.
[11] K. Sutter, G. Knöpfle, N. Saupper, J. Hulliger, P. Günter, J. Opt. Soc. Am. B 8 (1991) 1483.
[12] Anwar, S. Okada, H. Oikawa, H. Nakanishi, Chem. Mater. 12 (2000) 1162.
[13] J.M. Cole, J.A.K. Howard, G.J. McIntyre, Acta Crystallogr., Sect. B 57 (2001) 410.
[14] B. Borecka-Bednarz, A. Bree, B. Patrick, J. Scheffer, J. Trotter, Can. J. Chem. 76 (1998) 1616.
[15] T. Kolev, D. Yancheva, D.C. Kleb, M. Schurmann, H. Preut, P. Bleckmann, Z. Krist, NCS 216 (2001) 65.
[16] T.M. Kolev, D.Y. Yancheva, B.A. Stamboliyska, Spectrochim. Acta 59 (2003) 1805.
[17] T.M. Kolev, B.A. Stamboliyska, D.Y. Yancheva, V. Enchev, J. Mol. Struct. 191 (2004) 241.
[18] T.M. Kolev, D.Y. Yancheva, S.I. Stoyanov, Adv. Funct. Mater. 14 (2004) 799.
[19] T. Kolev, D. Yancheva, M. Schurmann, D.C. Kleb, H. Preut, M. Spiteller, Acta Crystallogr., Sect. E 58 (2002) o1267.
[20] T. Kolev, R. Wortmann, M. Spiteller, W.S. Sheldrick, H. Mayer-Figge, Acta Crystallogr., Sect. E 60 (2004) o1449.
[21] T. Kolev, D. Yancheva, B. Shivachev, R. Petrova, M. Spiteller, Acta Crystallogr., Sect. C 61 (2005) 213.
[22] T. Kolev, R. Wortmann, M. Spiteller, W.S. Sheldrick, H. Meyer-Figge, Acta Crystallogr., Sect. E 61 (2005) o1090.
[23] T. Kolev, R. Wortmann, D. Yancheva, unpublished work.
[24] M.J. Frisch, G.W. Trucks, H.B. Schlegel, G.E. Scuseria, M.A. Robb, J.R. Cheeseman, V.G. Zakrzewski, J.A. Montgomery Jr., R.E. Stratmann, J.C. Burant, S. Dapprich, J.M. Millam, A.D. Daniels, K.N. Kudin, M.C. Strain, O. Farkas, J. Tomasi, V. Barone, M. Cossi, R. Cammi, B. Mennucci, C. Pomelli, C. Adamo, S. Clifford, J. Ochterski, G.A. Petersson, P.Y. Ayala, Q. Cui, K. Morokuma, D.K. Malick, A.D. Rabuck, K. Raghavachari, J.B. Foresman, J. Cioslowski, J.V. Ortiz, A.G. Baboul, B.B. Stefanov, G. Liu, A. Liashenko, P. Piskorz, I. Komaromi, R. Gomperts, R.L. Martin, D.J. Fox, T. Keith, M.A. Al-Laham, C.Y. Peng, A. Nanayakkara, C. Gonzalez, M. Challacombe, P.M.W. Gill, B. Johnson, W. Chen, M.W. Wong, J.L. Andres, C. Gonzalez, M. Head-Gordon, E.S. Replogle, J.A. Pople, Gaussian 98, Revision A.7, Gaussian, Inc., Pittsburgh, PA, 1998.
[25] D. Becke, J. Chem. Phys. 98 (1993) 5648.
[26] C. Lee, W. Yang, R.G. Parr, Phys. Rev. B 37 (1988) 785.
[27] C. Peng, P.Y. Ayala, H.B. Schlegel, M.J. Frisch, J. Comp. Chem. 17 (1996) 49.
[28] A.P. Scott, L. Radom, J. Phys. Chem. 100 (1996) 16502.
[29] A. Schmidt, U. Becker, A. Aimene, Tetrahedron Lett. (1984) 4475.
[30] C. Reichardt, Solvents and Solvent Effect, in Organic Chemistry, VCH, Weinheim, Germany, 1990 (Chapters 6 and 7).
[31] T. Kolev, M. Schürmann, D.-C. Kleb, H. Preut, P. Bleckmann, Acta Crystallogr., Sect. E 58 (2002) o867.

[32] H. Yamamoto, T. Hosomi, T. Watanabe, S. Miyata, J. Chem. Soc. Jpn. Chem. Indust. Chem. 7 (1990) 789.
[33] H. Terao, Y. Itoh, K. Ohno, M. Isogai, A. Kakuta, A. Mikoh, Opt. Commun. 75 (1990) 451.
[34] J. Cioslowski, J. Am. Chem. Soc. 111 (1989) 8333.
[35] R. Wortmann, P. Krämer, C. Glania, S. Lebus, N. Detzer, Chem. Phys. 173 (1993) 99.
[36] R. Wotmann, C. Glania, P. Krämer, K. Lukaszuk, R. Matschiner, R.J. Twieg, F. You, Chem. Phys. 245 (1999) 107.
[37] F. Würthner, R. Wotmann, R. Matschiner, K. Lukaszuk, K. Meerholz, Y. DeNardin, R. Bittner, C. Bräuchle, R. Sens, Angew. Chem., Int. Ed. Engl. 36 (1997) 2765.
[38] Ts. Kolev, P. Bleckmann, Spectrosc. Lett. 23 (1990) 391.
[39] M. Szostak, T. Misiaszek, R. Roszak, J. Rankin, R. Czernuszewicz, J. Chem. Phys. 99 (1995) 14992.
[40] I. Juchnovski, Ts. Kolev, Spectrosc. Lett. 18 (1985) 481.
[41] M. Szafran, J. Koput, J. Mol. Struct. 381 (1996) 157.